Gene Expression Patterns 19 (2015) 120–128

Contents lists available at ScienceDirect

Gene Expression Patterns

journal homepage: http://www.elsevier.com/locate/gep

Spatial and temporal distribution of Patched-related protein in the *Drosophila* embryo

Carmen Bolatto [a], Cristina Parada [a], Fiorella Revello [a], Alejandro Zuñiga [b], Pablo Cabrera [b], Verónica Cambiazo [b, *]

[a] Laboratorio de Biología del Desarrollo, Departamento de Histología y Embriología, Facultad de Medicina-Universidad de la República, Montevideo, Uruguay
[b] Laboratorio de Bioinformática y Expresión Génica, INTA-Universidad de Chile and Fondap Center for Genome Regulation (CGR), Santiago, Chile

ARTICLE INFO

Article history:
Received 19 May 2015
Received in revised form
8 October 2015
Accepted 21 October 2015
Available online 23 October 2015

Keywords:
Drosophila
Patched-related
Hemocyte
Embryogenesis

ABSTRACT

Patched-related (*Ptr*) encodes a protein with 12 potential transmembrane domains and a sterol-sensing domain that is closely related in predicted topology and domain organization to Patched, the canonical receptor of the Hedgehog pathway. Here we describe the production of an antibody specific for *Drosophila* Ptr and analyse its spatial and temporal distribution in the embryo. We find that at early developmental stages Ptr is predominantly localized at cell periphery but later on it becomes strongly and almost exclusively expressed in hemocytes. Interestingly *Ptr* null mutant embryos died without hatching. Our findings suggest that Ptr plays an essential function in *Drosophila* development, perhaps as a new receptor of embryonic hemocytes.

1. Introduction

Seven classes of multipass transmembrane proteins carry a conserved domain known as sterol-sensing domain (SSD), which consists of about 180 amino acids that form 5 consecutive membrane spanning segments. This motif was initially identified in HMG CoA reductase (HMGCR) and SREBP cleavage activating protein (SCAP), two proteins involved in sterol synthesis and sterol-dependent transcription, respectively (Hampton, 2002). Subsequently additional proteins such as 7-dehydrocholesterolreductase (Witsch-Baumgartner et al., 2001), Niemann–Pick disease type C1 (NPC1) (Carstea et al., 1997), Patched (Ptc) (Hooper and Scott, 1989) and Dispatched (Disp) (Burke et al., 1999) with roles in cholesterol biosynthesis, lipid transport and transport of cholesterol-modified morphogen Hedgehog (Hh) have been shown to carry the SSD motif. More recently a group of membrane proteins named as Patched-related (Ptr), which is closely related in predicted topology to Ptc and Disp, were characterized in *C. elegans* (Kuwabara and Labouesse, 2002). The Ptr proteins seem to function in multiple aspects of development, including cell growth, patterning, and molting, a process that depends on the availability of sterols (Zugasti et al., 2005).

The SSD-containing proteins are found in a variety of organisms, in *Drosophila* a repertoire of SSD-containing proteins with structural and functional similarities to their vertebrate counterparts has been identified, highlighting the central importance of these proteins in variety of cellular processes, such as cholesterol homeostasis, vesicle trafficking, cell signalling and cytokinesis (Kuwabara and Labouesse, 2002). In an evolutionary sense, studies in *Drosophila* have provided insights on the ancestral function of SSD-containing proteins. For instance, in mammals activation of SREBP (sterol response element binding proteins) by SCAP is regulated by low levels of sterols, whereas in flies SCAP responds to palmitic acid (Seegmiller et al., 2002), suggesting that the original function of the SCAP-SREBP pathway may have been to maintain the integrity of the cell membrane.

A *Drosophila Ptr* gene (CG11212) was originally isolated in a subtractive hybridization screening designed to identify genes that

Abbreviations: SSD, sterol-sensing domain; HMGCR, HMG CoA reductase; SCAP, SREBP cleavage activating protein; NPC1, Niemann–Pick disease type C1; Ptc, Patched; Disp, Dispatched; Hh, Hedgehog; Ptr, Patched-related; SREBP, sterol response element binding proteins; GST, glutathione S-transferase; ECM, extracellular matrix; Crq, Croquemort; Pvr, PDGF/VEGF receptor.

* Corresponding author.
E-mail addresses: cbolatto@fmed.edu.uy (C. Bolatto), cristinap@fmed.edu.uy (C. Parada), fiorev85@gmail.com (F. Revello), jano@inta.uchile.cl (A. Zuñiga), vcambiaz@inta.cl (V. Cambiazo).

http://dx.doi.org/10.1016/j.gep.2015.10.002
1567-133X/

are differentially expressed at the beginning of gastrulation (Zuniga et al., 2009). We cloned the gene and deduced that the product is a 1061 amino acids protein closely related in predicted topology and domain organization to the protein encoded by the *Drosophila* segment polarity gene *ptc*. In addition, our biochemical analysis revealed that Ptr is associated with embryo membranes and immunohistochemistry analyses allowed us to localize this protein to the growing plasma membranes in *Drosophila* blastoderms and in vesicles-like structures of S2 cells overexpressing a Ptr-V5 fusion protein (Zuniga et al., 2009; Pastenes et al., 2008).

Here we describe the production of an antibody specific for *Drosophila* Ptr and analyse its temporal and spatial distribution in the embryo. In addition, we present an initial characterization of a null mutation in the *Ptr* gene, created by imprecise P-element excision. *Ptr* null mutant embryos died without hatching, indicating that Ptr plays an essential function in *Drosophila* development.

2. Results

2.1. Generation of antibody specific for Ptr protein

The spatial and temporal pattern of Patched-related expression has been only briefly reported (Pastenes et al., 2008) with antibodies no longer available, so a new polyclonal antiserum against a 275 amino acids peptide from the carboxyl termini of Ptr (aa 855 to 1129) was generated. The quality of the signal displayed by the new anti-Ptr antibody, was first tested by Western blot assays using a purified recombinant Ptr protein consisting of the 275 amino acids peptide fused to a poly-His tag (Fig. 1, lane A). Then, Western blot assays were performed using lisates of cl-8 cells that overexpress a Ptr-V5 construct under the control of an inducible metallothionein promoter (see Sections 4.2–4.4). To confirm the specificity of the signal, these experiments included as control the use of a monoclonal anti-V5 antibody to recognize the protein tag. The results showed that both the polyclonal anti-Ptr and the monoclonal anti-V5 antibodies recognized a single band at 95 kDa (Fig. 1 left, lanes B and C). The apparent molecular weight of Ptr was different to that predicted by its sequence (120 kDa). This biochemical behaviour, termed “gel shifting”, was reported previously in other studies and appears to be frequent for membrane proteins (Rath et al., 2009; Nybo, 2012). The origin of gel shift behaviour might derive from altered binding caused by the detergent. In our experiment, the need to avoid boiling the sample to prevent protein aggregation conspired against the uniform binding of SDS to the sample proteins. Nevertheless, the correspondence of the 95 kDa signal to Ptr was confirmed by the co-staining with anti-V5 antibody. Uninduced cells were used as control to confirm the absence of reactivity with anti-Ptr antibody (Fig. 1 left, lane D). In addition, transfected cl-8 were processed for immunofluorescence using the anti-Ptr and anti-V5 antibodies (green and red signal, respectively). Ptr and V5 signals colocalized in vesicle-like structures (Fig. 1, right). The specificity of the anti-Ptr antiserum was further demonstrated by the absence of immunostaining in a *Ptr* null mutant embryos (see Section 2.3). Thus, we concluded that the antiserum generated specifically recognized the Ptr protein.

2.2. Expression pattern of Ptr during Drosophila embryogenesis

The structural similarities of Ptr and Ptc along with the association of Ptr with embryo membranes (Zuniga et al., 2009; Pastenes et al., 2008) prompted us to compare the expression pattern of Ptr and Ptc at early and late stages of embryogenesis. To do this, we performed double immunofluorescence analyses by staining embryos with anti-Ptr and anti-Ptc antibodies. The spatial distribution of Ptc protein observed here was consistent with that reported previously (Capdevila et al., 1994; Taylor et al., 1993) allowing us to compare it with that of Ptr.

In early embryos (cellular blastoderm and gastrula stages) the immunofluorescence signals of Ptr and Ptc showed a uniform distribution in almost all cells (Fig. 2 A–L). As previously showed (Pastenes et al., 2008), Ptr is distributed around the periphery of the cell and accumulates in cytoplasmic dots (Fig. 2 D–F). This

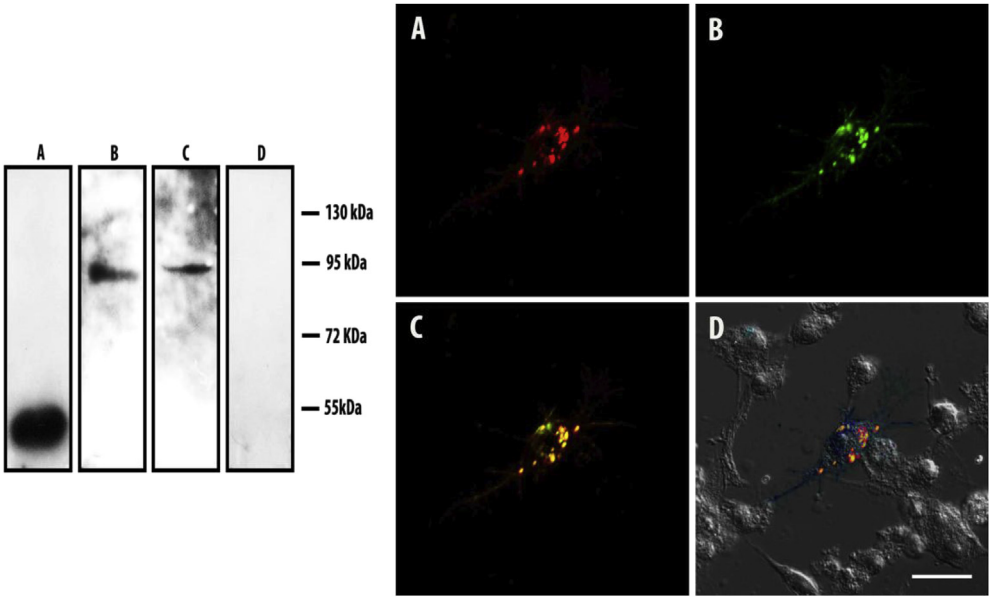

Fig. 1. Polyclonal anti-Ptr antibody specifically recognizes recombinant Ptr proteins. Left panel, anti-Ptr detected the presence of Ptr recombinant protein (lane A). A lysate of cl-8 cells induced to express Ptr-V5 was used as sample in western blot analysis. Monoclonal anti-V5 (lane B) and polyclonal anti-Ptr (lane C) antibodies detected a coincident signal at 95 KDa in the lysate. A lysate of uninduced cells was used as a control and probed with the anti-Ptr antibody (lane D). Right panel, overexpression of Ptr-V5 in cl-8 cells was verified by immunostaining using the same antibodies mentioned above. Both, anti-V5 (red in A) and anti-Ptr (green in B) showed a similar signal. Colocalization of signals was corroborated in the merged image (yellow in C). Cells were visualized using Nomarski microscopy (D). Scale bar: 10 μm.

subcellular arrangement is reminiscent to that described for Ptc. Ultrastructural localization of anti-Ptr using electron microscopy and a pre-embedding immunogold method demonstrated that Ptr is associated to vesicular and plasma membranes (Fig. 2G–I). At stage 12 of embryogenesis when germ band shortening takes place, Ptc is expressed in 15 alternating stripes over the trunk region (Capdevila et al., 1994), whereas the anti-Ptr antibody stained conspicuous zones with high concentration of the protein (Fig. 2 M–U) that were not coincident with the Ptc-positive stripes. During germ band shortening, distribution of Ptr positive cells was reminiscent of the spatial pattern of migrating hemocytes. Thus, Ptr positive cells were concentrated at both ends of the embryo (Fig. 2N, arrows) from where they migrated towards the middle of the embryo. Migration took place along different paths that were highly coincident with those previously described as the sterotyped paths of hemocyte migration: ventral surface of ventral nerve cord (vs), dorsal surface of ventral nerve cord (ds) and dorsal epidermis (de) (Fig. 2Q and T). There is a fourth path followed by hemocytes during migration, but it is inside the embryo, surrounding the gut and it was nor clearly visible in our inmmunofluorescence stainings (Evans et al., 2010; Wood and Jacinto, 2007; Tepass et al., 1994). At a later stage of development Ptr positive cells were observed around the brain (Fig. 2W, arrowheads) and bilaterally around the amnioserosa (Fig. 2W, as).

In order to verify whether Ptr staining was enriched in the hemocyte population of cells, (Evans et al., 2010; Olofsson and Page, 2005) embryos expressing UAS-*lacZ* under the control of hemocyte-specific GAL4 driver (*crq*-GAL4) were immunostained using anti-Ptr and anti-beta galactosidase (beta-gal) antibodies (Fig. 3). We found that the patterns of immunostaining for beta galactosidase and Ptr were highly similar, indicating that Ptr is enriched in the hemocytes at late stages of embryonic development. Although expression pattern of *lacZ* driven by *crq*-GAL4 was according to previous descriptions (i.e. starts at germ band retraction stage), the overlap between anti-Ptr and anti-beta-gal signals was incomplete and denoted a potential subset of Ptr positive embryonic macrophages. The specificity of the Ptr staining in blood cells was confirmed by the absence of immunofluorescence in *Ptr* null mutant embryos (Fig. 4).

2.3. Generation of a Ptr mutant and antibody validation

We searched the Flybase for P-element insertion lines near *Ptr* gene and identified the line PSUPor-PKG01682 in which the PSUPor-P element (Bellen et al., 2004) was adjacent to the predicted 5′-UTR of *Ptr*. The line was homozygous viable lacking an obvious mutant phenotype. To identify the complete 5′-UTR of *Ptr* gene, we performed a 5′ Race using embryos at stage 5. Sequencing of the 5′ Race PCR products revealed two 5′-UTR sequences, 5′-UTR 1 (357 bp) and 5′-UTR 2 (614 bp) (data not shown). Based on EST (expressed sequence tag) sequence data, the 5′-UTR 1 appears to be predominantly transcribed (FlyBase, http://flybase.bio.indiana.edu). This result allowed us to map the insertion site of the P-element 335 bp 5′ of the 5′-UTR 1. To obtain mutants for *Ptr* we mobilized the P element in a standard cross with the Δ2–3 strain, which stably expresses transposase (Robertson et al., 1988), then flies were generated and selected in which imprecise excision events eliminated the P-element. We recovered one excision line (23C) that was homozygous lethal, the extent of the genomic deletion is shown in Fig. 4A. Line 23C has a deletion of 3852 bp removing the transcription start site and 1212 bp encoding the 5′-UTR and part of the first intron of the gene. In the 23C line the neighbouring gene CG30432 is completely deleted. CG30432 is reported as a gene moderately expressed in imaginal discs and testis, with very low or no expression during embryonic development (Graveley et al., 2011), suggesting that the observed lethality could be caused by the mutation in *Ptr*.

To test whether this deletion efficiently affected the expression of *Ptr*, PCR assays were performed using a pair of primers that annealed with exons 3 and 7 of *Ptr*. Amplification products were not recovered when the cDNA of homozygous mutant embryos from line 23C was used as substrate, whereas fragments of correct sizes were detected when genomic DNA or cDNA from wild type embryos were used as substrates for the PCR reactions (Fig. 4B). In addition, line 23C was balanced with a marked balancer chromosome to distinguish homozygous mutant embryos by their lack of GFP expression (see Section 4.6) (Casso et al., 1999). With the help of this tool we determined that all the homozygous *Ptr* null embryos (i.e. GFP negative) died before or short time after hatching. Therefore, we conclude that a null mutation for *Ptr* gene (Ptr^{23C}) was obtained. Using the Ptr^{23C} line the newly generated anti-Ptr antibody was validated by an absence of signal in the *Ptr* null mutant (Fig. 4C–F). As a first step to characterize the Ptr^{23C} line, we examined the presence of hemocytes in wild type and *Ptr* mutant embryos using an anti-fascin antibody that labels the subpopulation of migrating hemocytes (Zanet et al., 2009). Differences could be detected in the number and distribution of migrating hemocytes between wild type (Fig. 5A) and Ptr^{23C} embryos (Fig. 5B).

3. Discussion

Previous work indicate that Ptr displays a similar structure and topology with Ptc, a negative regulator of the Hh pathway (Taipale et al., 2002; Chen and Struhl, 1996; Ingham et al., 1991). Here, we showed that Ptc and Ptr display distinctive expression patterns during embryogenesis. At early stages, Ptr and Ptc immunoreactivity seem to be predominantly associated to cell membranes. At later stages, when Ptc-positive stripes are formed, Ptr becomes highly enriched in the migrating hemocytes. According to the temporal transcriptome of *Drosophila* published by the modENCODE project (Graveley et al., 2011) the transcription profile of Ptr shows a sharp increment from mid-embryogenesis, co-temporal with hemocyte differentiation and migration as phagocytic cells (Tepass et al., 1994). This is consistent with our findings of strong Ptr immunoreactivity in hemocytes at this stage. In this regard, Ptr immunostaining in embryos expressing UAS-*lacZ* under the control of the *crq*-GAL4 driver showed that a subset of migrating hemocytes expressing beta-galactosidase coexpressed Ptr, suggesting the existence of a subset of Ptr-positive cells. To our knowledge, distinct subsets of cells have not been characterized among migrating hemocytes, although the expression of a Tn antigen, with putative roles in immune response, has been detected in a subgroup of embryonic hemocytes (Yoshida et al., 2008).

Hemocytes are circulating cells responsible for the phagocytosis of apoptotic cells in *Drosophila* and other invertebrates. During embryogenesis, hemocytes carry out essential functions within the embryo, in addition, they are important for embryonic tissue formation as well as organ remodelling during metamorphosis (Tepass et al., 1994; Franc et al., 1996; Abrams et al., 1993; Franc et al., 1999). The ability of the hemocytes to recognize, migrate towards and engulf dying cells is controlled by transmembrane proteins acting as receptors. For example Croquemort (Crq), a member of the CD36 family of proteins, is a *Drosophila* macrophage receptor with roles in the binding and clearance of apoptotic cells in *Drosophila* embryos (Franc et al., 1996). Another receptor that is involved in apoptotic engulfment is Draper that functions in phagocytosis of apoptotic cells by migrating hemocytes (Manaka et al., 2004). On the other hand, the PDGF/VEGF receptor (Pvr) is part of the mechanism of hemocyte migration, directing hemocyte precursors along stereotyped migratory routes (Heino et al., 2001;

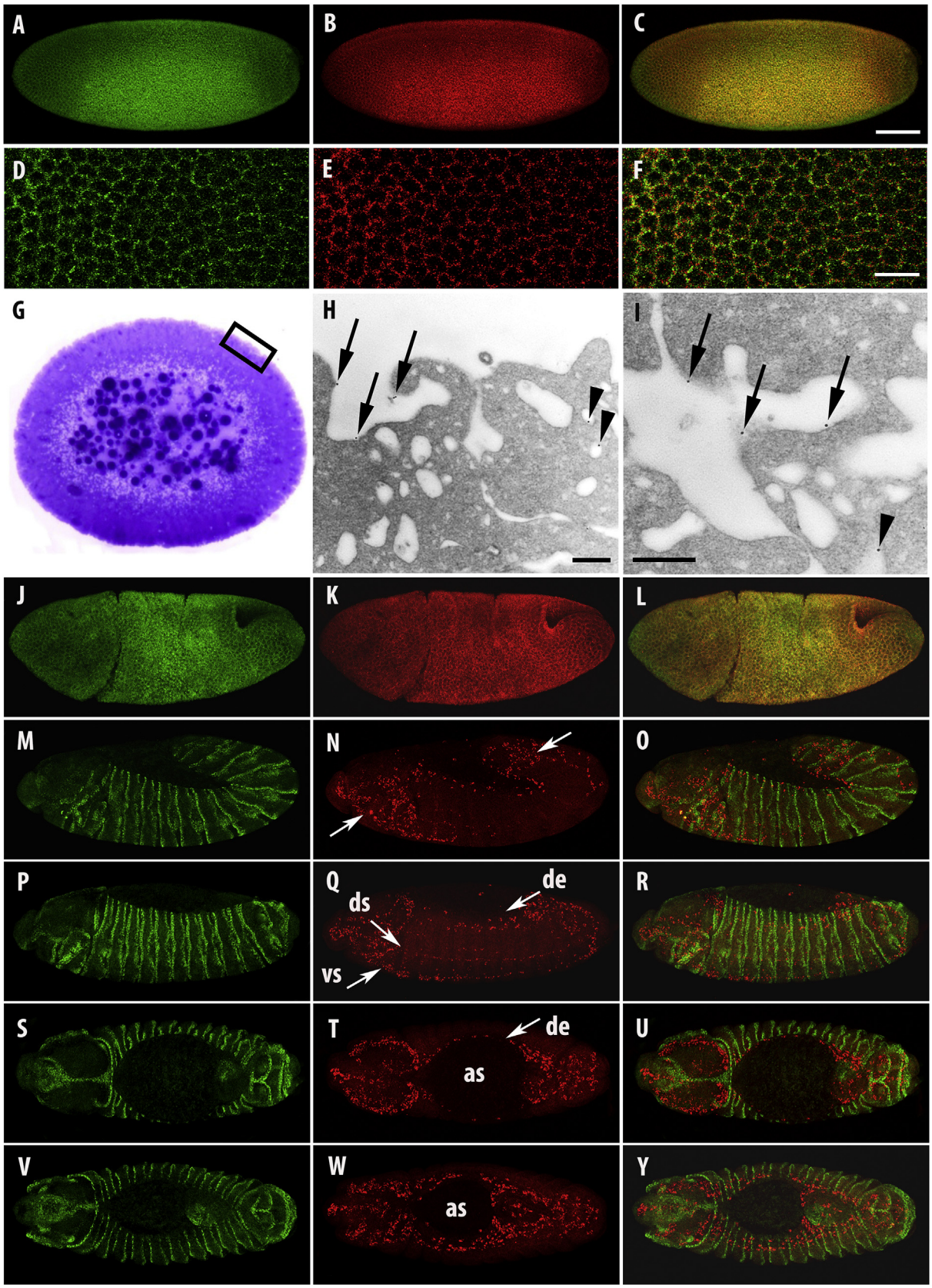

Fig. 2. Expression pattern of Ptr during *Drosophila* embryogenesis. Confocal microscopy images of whole-mount wild-type embryos double stained for Ptc (green signal: A, D, J, M, P, S, V) and Ptr (red signal: B, E, K, N, Q, T, W)). Yellow indicates signal overlaping in the merged images (C, F, L, O, R, U, Y). (A–C) Stage 5 embryo (blastoderm cellularization), (D–F) Higher magnification images of blastoderm stage to show similar distribution of the two proteins. (G–I) Pre-embedding immunogold using anti-Ptr to show the association of the protein with plasmatic (arrow) and vesicular (arrowhead) membranes at blastoderm stage. Magnified area in H and I is outlined in G by a black rectangle. (J–L) Stage 7 embryo (gastrulation), (M–U) Stage 12 embryo (germ band shortening), (V–Y) Stage 13 embryo (completion of germ band shortening). (A–B and J–R) Lateral and (S–Y) ventral views. At late stages of embryogenesis the antibody detected conspicuous zones with high concentration of Ptr. The distribution of these zones is coincident with some of the sterotyped paths of hemocyte migration: ventral surface of ventral nerve cord (vs), dorsal surface of ventral nerve cord (ds), dorsal epidermis (de), around the brain and around the amnioserosa (as). Scale Bars: (C) 50 μm, (F) 10 μm and (H–I) 500 nm.

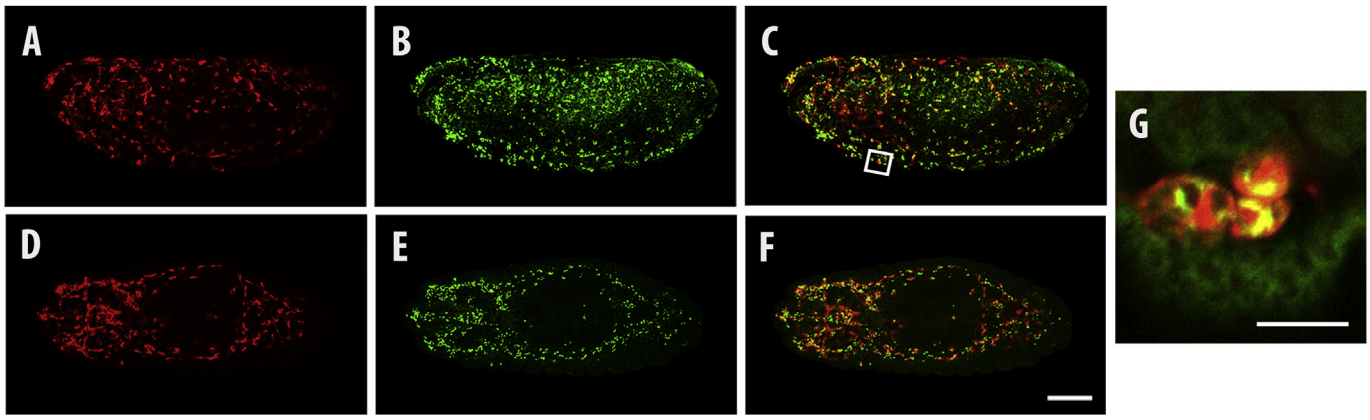

Fig. 3. Ptr is expressed in embryonic macrophages. Confocal images of *Drosophila* embryos at stage 13/14, viewed (A–C) laterally or (D–F) dorsally with the anterior end to the left of the panel. The expression pattern of the *lacZ* gene product under control of the macrophage driver *crq*-GAL4 (red signal: A, D) indicated that Ptr (green signal: B, E) accumulates in hemocytes. (C and F). Merged images indicate signal co-localization (yellow) in the entire embryo (C, F) or in a region close to its dorsal surface (G) to show hemocytes placed in the ventral surface of ventral nerve cord. Magnified area (G) is outlined in C by a white rectangle. Scale bars: (F) 50 μm and (G) 20 μm.

Cho et al., 2002; Wood et al., 2006). In addition, it is relevant to promote the survival of blood cells in the embryo. Thus, Pvr mutant embryos have large numbers of apoptotic hemocytes and drastically reduced total hemocyte number. Interestingly, the absence of Ptr also seems to affect the number of the migrating hemocytes at least at late stages of embryogenesis, suggesting that the lack of Ptr alters cell proliferation or induces hemocyte apoptosis. Further studies will be necessary to determine the role of Ptr on the development and differentiation of embryonic hemocytes.

Although it has been detected a close correlation between the pattern of apoptosis an the migratory routes travelled by hemocytes in the embryo (Tepass et al., 1994; Abrams et al., 1993), it is not clear how morphogenetic processes are able to coordinate developmental migrations with hemocyte homing toward dying cells along sterotyped migration pathways and how hemocytes are able to sense apoptotic cells at a distance (Wood and Jacinto, 2007; Cho et al., 2002). Thus, hemocytes have to respond to a diversity of signals arriving from extracellular matrix (ECM) or from other cells to perform vital functions: the clearance of apoptotic cells and the deposition of ECM. Because receptors and intracellular pathways activated by such signals are still partially known, it is attractive for us to trace the presence of Ptr, a transmembrane protein, to the migrating hemocytes.

Hemocyte malfunction has been related with alterations in the intestine and nervous system (Brown, 1994; Yarnitzky and Volk, 1995; Schmid et al., 2002; Sears et al., 2003). Future studies will clarify the existence of such malformations in *Ptr* null embryos. In this sense, the observation that these mutant embryos fail to hatch from the vitelline membrane encouraged us to define future experiments to evaluate the deposition level of ECM components. Because somatic muscle contraction is important for the embryos to hatch from the eggshell (Wright, 1960; Stronach et al., 1999) and hemocytes lay down much of ECM in the embryo (Fessler and Fessler, 1989; Cecchini et al., 1987; Mirre et al., 1988; Kusche-Gullberg et al., 1992; Yasothornsrikul et al., 1997; Le Parco et al., 1986; Fogerty et al., 1994), it would be of interest to determine whether *Ptr* null mutant embryos show alterations in somatic muscle attachment.

In summary, our results help to determine the expression pattern of Ptr, a SSD-containing protein whose role in the development has not yet been established. It was demonstrated that at later stages of embryogenesis, Ptr protein was highly expressed in a hemocyte-specific pattern. In addition, lack of Ptr seems to affect the number and distribution of hemocytes. These observations were unexpected and encourages us to delineate more sophisticated functional investigations to elucidate the role of Ptr in these cells.

4. Experimental procedures

4.1. Production of Ptr anti-serum

To generate the Ptr-GST fusion protein, an 825 bp fragment of Ptr, encompassing residues 855 to 1129, was cloned into a pGEX-6P-1 vector (Amersham Biosciences). The construct was then used to transform BL21 competent cells. An overnight culture of bacteria carrying the fusion protein construct was inoculated (1:100 dilution) into 200 ml of LB plus ampicillin. Expression of the fusion protein was induced by the addition of IPTG to a final concentration of 1 mM and culture was growth 1 h at 37 °C. The bacteria were harvested by cold centrifugation (4 °C) at 8000× g for 10 min. The pellet was resuspended in 10 ml of phosphate buffered saline (PBS) with protease inhibitors and sonicated on ice (ten times for 10 s each, with 1 min rest between sonications). Then, TritonX-100 was added to a final concentration of 1%, the mix was incubated for 20 min and centrifuged at 12,000× g (4 °C) for 20 min. Examination of Coomassie blue stained gels revealed that after induction of bacteria transformed with pGEX constructs, the 275 amino acids Ptr peptide was expressed as part of a GST fusion protein. The GST fusion protein was purified using Glutathione Superflow resin (Qiagen) according to the manufacturer's instructions. The release of the recombinant polypepetide from its GST tag was performed by on-column procedure using PreScission protease (GE Healthcare). After the cleavage, the product was dialysed using Amicon (molecular weight cutoff 30 kDa, EMD Millipore) and employed to immunize a rabbit. Freund's complete and incomplete adjuvants were used for the primary immunization and for subsequent boosts, respectively. After several boosts, the presence of antibodies specific for Ptr was detected in the serum of this animal by Western blot (data not shown). Finally, the serum was affinity purified against Ptr fusion protein without GST. In western blot analysis the antibody was used at a dilution 1:1000 whereas in immunofluorescence the same antibody was used at a dilution 1:100.

The same 825 bp fragment of Ptr was PCR amplified and cloned into pTrcHis2Topo vector (Invitrogen). The resulting histidine-tagged protein was purified using Ni-NTA agarose (Invitrogen) according to the manufacturer's instructions and employed as positive control on western blot studies.

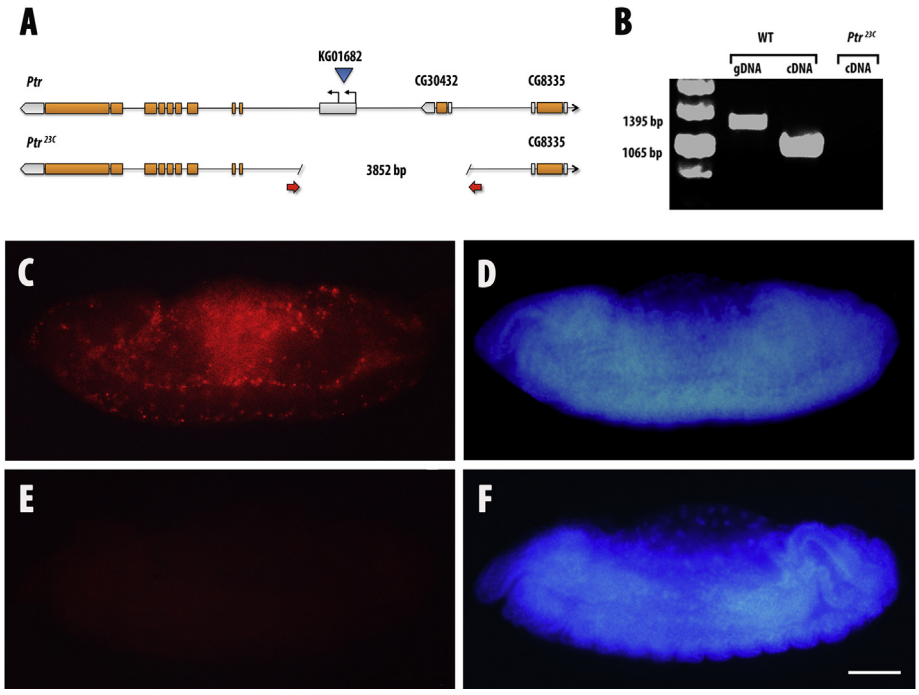

Fig. 4. *Ptr*-null mutant embryos lack of anti-Ptr immunoreactivity. (A) Schematic representation of the *Ptr* genomic region. The intron-exon structures of *Ptr* and two adjacent genes, CG30432 and CG8335, depicting translated regions (orange bars) and untranslated regions (grey bars) are indicated. Ptr transcriptional start sites are indicated by arrows. The blue triangle indicates the site of the PSUPor-P element insertion, from which the line Ptr^{23C} was generated by imprecise excision. The extent of the deletion is indicated by red arrows. (B) To detect *Ptr* transcripts RT-PCR assays were performed using cDNA samples from wild type (WT) or Ptr^{23C} mutant embryos and a pair of primers that annealed with exons 3 and 7 of *Ptr*. (Ptr ex3-s and Ptr ex7-a in Table 1). Using the same primers, genomic DNA (gDNA) from wild type embryos was also amplified. In wild type embryos *Ptr* transcripts were present whereas in Ptr^{23C} mutant embryos the transcripts were absent. (C and D) Lateral views of a wild type stage 14 embryo stained with anti-Ptr (red) and DAPI (blue). Ptr protein can be detected predominantly in hemocytes. (E and F) Lateral views of *Ptr*-null mutant embryos at similar developmental stage stained with anti-Ptr and DAPI, respectively. Anti-Ptr staining can not be detected in Ptr^{23C} mutant embryos. Scale Bar: 50 μm.

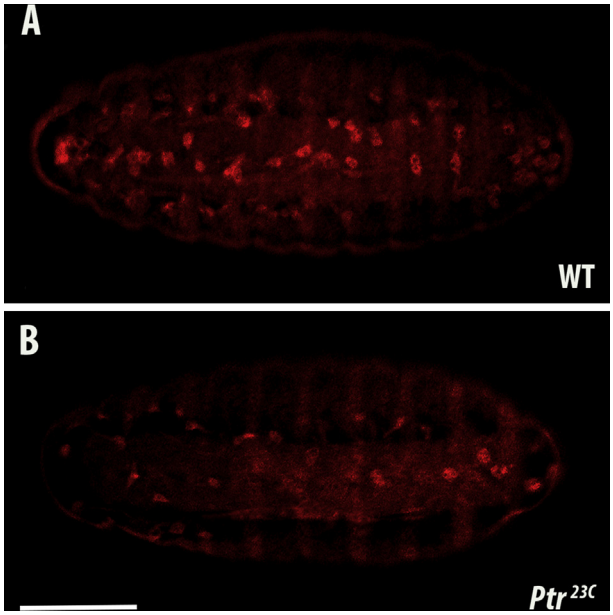

Fig. 5. Hemocytes detection in wild type and Ptr^{23C} embryos. Whole mounts of wild type (A) and Ptr^{23C} (B) embryos at stage 15/16 stained with anti-fascin antibody which labels hemocytes, epidermal cells and central nervous system. Images correspond to ventral views of embryos with the anterior end to the left. Homozygous mutant embryos were distinguished by the lack of *lacZ* product detection in double immunofluorescence assays with an anti-beta galactosidaes antibody. Scale bar: 50 μm.

4.2. Cell cultures and transfection

Cl-8 cells (obtained from the *Drosophila* Genomics Resource) were cultured in Shields and Sang M3 insect medium (Sigma) supplemented with 2% heat-inactivated fetal bovine serum, 2.5% fly extract, 0.5 mg/ml insulin and antibiotics. To overexpress Ptr, cells were transfected with 2 μg of pMT/V5-His-Topo (Invitrogen) vector containing the coding sequence of gene *Ptr* (residues 1 to 1129) using Calcium phosphate transfection kit (Invitrogen) according to the manufacturer's instructions. Expression of the constructs was induced 48 h post-transfection by adding $CuSO_4$ to the cell medium (final concentration 0.5 mM). After 24 h, induced and uninduced (control) cells were harvested, transferred onto coverslips, and fixed with 4% paraformaldehyde.

4.3. Cell lysate and western blotting

Cell extract was obtained by lysing with 600 μl cold lysis buffer (20 mM Tris, pH 7.5, 150 mM NaCl, 1 mM EDTA, 1 mM EGTA, 1% Triton X-100 and protease inhibitor cocktail) three 60 mm culture dishes of cl-8 cells induced or uninduced with $CuSO_4$ to express Ptr-V5. The lysate was centrifuged for 10 min at 16,000× *g* at 4 °C and the supernatant was stored at −80 °C. Protein determination was performed on aliquots using Bradford reagent (Fermentas). To detect the presence of Ptr-V5, 16 μg of the cell lysate was separated by SDS-PAGE and transferred to PVDF membrane for 2 h at 100 V. Before loading the gel, the samples were incubated with Laemmli sample buffer 30 min at 37 °C (not boiled) to avoid the formation of protein aggregates. The membrane was blocked (5% low-fat milk in Tris-buffered saline pH 7.4) for 1 h at room temperature and

incubated for 16 h at 4 °C with rabbit anti-Ptr or mouse anti-V5 (Santa Cruz Biotechnology) antibodies diluted 1:1000 and 1:100. To detect the primary antibodies, anti-rabbit or anti-mouse secondary antibodies conjugated to peroxidase were used (Thermo Scientific).

4.4. Immunostaining of cells and embryos

Cells were fixed with 4% paraformaldehyde, permeabilized with PBS containing 0.1% Triton X-100 for 15 min, and then incubated in blocking buffer (3% BSA 0.1% Triton X-100 in PBS) for 45 min prior to incubation with primary antibodies: monoclonal anti-V5 (1:500, Sigma) and polyclonal anti-Ptr (1:100). Cells were washed three times in PBS plus 0.1% Triton and incubated with the secondary antibodies and probes: anti-mouse Alexa 488 (Molecular Probes, 1:800), anti-rabbit Alexa Fluor 546 (Molecular Probes, 1:800) and DAPI (Molecular Probes, 1:5000).

Embryos of all stages were collected from grape juice agar plates and dechorionated (50% commercial bleach solution in PBS, 0.05% Triton X-100). Embryos were staged, fixed in a 1:1 (v/v) mixture of n-heptane and 4% formaldehyde for 30 min, and their devitellinisation was performed by the hand-peeling procedure. Embryos were then postfixed in 4% paraformaldehyde (Sigma–Aldrich) for 20 min, incubated at 4 °C for 30 min in blocking buffer (3% BSA, 0.1% Triton X-100, 50 mM glycine in PBS), and then incubated with Ptr affinity purified antibody (diluted 1:100) or anti-Ptc (Apa1, Development Studies Hybridoma Bank-DSHB, diluted 1:100) or anti-fascin (sn 7C, DSHB, diluted 1/20) or anti-β-galactosidase (Hybridoma Bank, diluted 1:10 or eBioscience, diluted 1:400). After overnight incubation at 4 °C the embryos were washed four times (15 min each) with blocking buffer and incubated for 1 h with anti-mouse Alexa Fluor 488 (1:800, Molecular Probes) or anti-rabbit Cy3 antibodies (1:1000 Jackson ImmunoResearch). DAPI (1:5000, Molecular Probes) was added together with the secondary antibodies to stain the nuclei. Digital images were captured with laser confocal microscopy using either a Leica TCS-SP5-DMI6000 or a Nikon C2 Plus-SiR microscope.

4.5. Electron microscopy

Embryos were collected and fixed for 1 h in a 1:1 mixture of heptane and freshly prepared 4% paraformaldehyde (Fluka) in PBS (pH 7.3) at room temperature. Then, embryos were manually devitellinized in PBS, transferred again to fixative for 30 min, washed in PBS and incubated in 3% BSA, 0.03% saponin and 1% goat serum in PBS for 40 min (two changes). The embryos were incubated with anti-Ptr antibody diluted 1/20 in the same buffer and incubation was performed for 16 h at 4 °C. Then, embryos were washed and incubated with secondary antibodies conjugated to 15 nm colloidal gold particles (anti-rabbit, EMS) in the same buffer for 1 h at room temperature. The embryos were then washed in PBS plus 0.03% saponin and incubated for 60 min, post-fixed in 2.5% glutaraldehyde (Fluka) in PBS for 10 min and washed again using PBS and stained overnight at 4 °C with 2% uranyl acetate (Merck). Then, the samples were dehydrated through an acetone series and embedded in Araldite for sectioning. Thin sections were obtained with a RMC MT–X ultramicrotome, stained with lead citrate, observed under a JEOL JEM-1010 transmission electron microscope and photographed using Hamamatsu Digital Camera CCD 4742–95.

4.6. Drosophila strains and genetic manipulations

All *Drosophila* stocks were maintained and crossed at 25 °C according to standard procedures. The *Ptr* mutant lines were generated by imprecise excision using the following stocks: w^{67c23}; P{$y^{+mDint2}$, $w^{BR.E.BR}$ = SUPor-P}KG01682 (P element line), w^*; wg^{Sp-1}/*CyO*; ry^{506}, Dr^1, P{$ry^{+t7.2}$ = Delta2-3}99B/*TM6* (transposase line), wg^{Sp-1}, J^1, L^2, Pin^1/*CyO*,P{$ry^{+t7.2}$ = *ftz*/*lacB*}E3 (CyO balancer line). The primer sequences used to characterize the deletion are described in Table 1. For lethal phase determination we balanced Ptr alleles over CyO, *kr*–GFP balancer gently donated by R. Cantera. Each mutant line was crossed with wild-type (Canton-S strain) flies. Males and females heterozygous for the mutation (Ptr^{23C}/+) were subsequently crossed to each other. Embryonic hemocytes were detected using embryos from a cross between y^1 w^*; P{$w^{[+mC]}$ = *crq*-GAL4} 2 (*crq*-GAL4) and w^{1118} w^*; P{UAS-*lacZ-B*}Bg4-2-4b (UAS-lacZ). All the stocks were obtained from the Bloomington Stock Center.

4.7. Rapid Amplification of cDNA Ends (RACE)

The 5'-end of the Ptr transcript was amplified using the RLM-RACE GeneRacer™ kit, according to the manufacturer's instructions (Invitrogen Carlsbad, CA). Briefly, 5 μg of total RNA from *Drosophila melanogaster* stage 5–7 embryos was used as starting material. The adaptor-ligated cDNA was PCR amplified using Platinum® Taq DNA Polymerase (Invitrogen Carlsbad, CA), GeneRacer™ 5′ Primer and 10 μM of gene-specific primer RACE11212-a2 under the following conditions: 2 min at 94 °C, 5 cycles of 30 s at 94 °C and 40 s at 72 °C, 5 cycles of 30 s at 94 °C and 40 s at 70 °C and 25 cycles of 30 s at 94 °C, 30 s at 65 °C and 40 s at 68 °C. The resulting PCR products were used in a Nested PCR reaction with GeneRacer™ 5′ Nested Primer and the gene-specific primer RACE 11212-a1 (see primer sequences in Table 1). The Nested PCR program comprises 2 min at 94 °C and 25 cycles of 30 s at 94 °C, 30 s at 65 °C and 2 min at 68 °C. The PCR products were cloned into pGEM-T Easy vector and sequenced.

4.8. Embryo genotyping

The method for genotyping was described by Ghanim and White (Ghanim and White, 2006). Briefly, heterozygous fly lines carrying the *Ptr* mutation were allowed to lay eggs on grape agar plates for 1 h. The collected embryos were dechorionated in 50% bleach and staged under light microscope. To perform RNA extraction of 10–15 homozygous embryos, one hundred embryos in stage 5 of development were selected and individually transferred into PCR tube containing 14.5 μl of extraction buffer (100 mM Tris–HCl pH8.2, 1 mM EDTA and 25 mM NaCl). After homogenization with a pipette tip, 11 μl from each single embryo extract were individually stored in a new tube containing 30 μl of RNA_{WIZ} reagent from Ambion (Austin, TX, USA) and frozen (−20 °C) to preserve RNA integrity. The remaining extract (3.5 μl) was incubated at

Table 1
Primers used in this study.

Primers used to characterize the deletion			
Name	Length (bp)	Tm (°C)	Sequence (5′ 3′)
UpPtr2-s	1853	62	GTTTTTCTGGGCTCAGTCGG
UpPtr5-as		60	CACGCAGGTCTTGTTTGAAG
UpPtr3-s	1637	62	GCGGCGAAGACAATGAGAGA
UpPtr4-as		60	TTGGAGTCCGAGTTAAGCCT
Primers used in RT-PCR and RACE analyses			
Name	Length (bp)	Tm (°C)	Sequence (5′ 3′)
Ptr ex3-s	1395 gDNA	72	AACAGACATTGGCTGGACAC
Ptr ex7-a	1065 cDNA	72	TTCGGGCGAGTCATTGTGA
RACE 11212-a1		72	TCGTTATGCGTCCGACGTTAAAGC
RACE 11212-a2		72	ACGTATAGGTATCACCATCATAAGTG

28 °C for 30 min with 200 μg/ml of proteinase K (Sigma–Aldrich, St. Louis, MO, USA), followed by incubation at 95 °C for 2 min. After the incubation with proteinase K the extract was used in PCR. In our case, absence of *lacZ* or GFP specific band together with the presence of a control band (gene CG9650) were indicators of homozygous lethal embryos.

4.9. RNA extraction

Extracts of homozygous mutant staged embryos preserved in RNA_{WIZ} reagent (N = 10 to 15) were pooled adding 300 μl of the reagent. To perform adequate tissue disaggregation, the samples were carefully homogenized in a 1.5 ml Eppendorf tube on ice with the aid of RNAse-free polypropylene pellet pestle. After complete the volume of each sample up 1 ml with RNA_{WIZ}, RNA extraction was performed using standard protocols. To increase the recovery of RNA, precipitation was made with the addition of glycogen (Ambion, Austin, TX, USA) to the isopropanol step. After 15 min of centrifugation at 13,000× *g*, RNA quality and quantity was evaluated by spectrophotometry (OD260/280) and by electrophoresis (1.2% formaldehyde-agarose gel). Samples were treated with TURBO DNA-free DNase (Ambion, Austin, TX, USA) to remove contaminating DNA.

Acknowledgements

We would like to thank Soledad Astrada, Lucía Guggeri, Lucía Pastro and Fiorella Scandroglio for their technical assistance; Beatriz Garat and Rafael Cantera for their advice and critical comments during this work; and the Bloomington *Drosophila* Stock Center for providing stocks used in this study. The Apa1 monoclonal anti-Ptc developed by Isabel Guerrero, the 40-1a monoclonal anti-Galactosidase developed by Joshua Sanes and sn 7C monoclonal anti-fascin developed by Lynn Cooley were obtained from the Developmental Studies Hybridoma Bank (DSHB) under the auspices of the NICHD and maintained by The University of Iowa, Department of Biological Sciences, Iowa City, IA 52242. Some materials were received through the Drosophila Genomics Resource Center. This work was supported by CSIC I+D 2010 to CB and Fondecyt N°1120254 to VC. CP and FR were supported by CSIC I+D 2010. AZ was supported by Postdoctoral Fondecyt N° 3110147. CB was also supported by fellowships from: CSIC (Programa de Recursos Humanos), PEDECIBA, AMSUD-Pasteur (Regional Training Fellowship Program) and Proyecto 720 (Contrapartida Convenios-UdelaR).

References

Abrams, J.M., White, K., Fessler, L.I., Steller, H., 1993. Programmed cell death during Drosophila embryogenesis. Development 117 (1), 29–43.
Bellen, H.J., Levis, R.W., Liao, G., He, Y., Carlson, J.W., Tsang, G., Evans-Holm, M., Hiesinger, P.R., Schulze, K.L., Rubin, G.M., et al., 2004. The BDGP gene disruption project: single transposon insertions associated with 40% of Drosophila genes. Genetics 167 (2), 761–781.
Brown, N.H., 1994. Null mutations in the alpha PS2 and beta PS integrin subunit genes have distinct phenotypes. Development 120 (5), 1221–1231.
Burke, R., Nellen, D., Bellotto, M., Hafen, E., Senti, K.A., Dickson, B.J., Basler, K., 1999. Dispatched, a novel sterol-sensing domain protein dedicated to the release of cholesterol-modified hedgehog from signaling cells. Cell 99 (7), 803–815.
Capdevila, J., Pariente, F., Sampedro, J., Alonso, J.L., Guerrero, I., 1994. Subcellular localization of the segment polarity protein patched suggests an interaction with the wingless reception complex in Drosophila embryos. Development 120 (4), 987–998.
Carstea, E.D., Morris, J.A., Coleman, K.G., Loftus, S.K., Zhang, D., Cummings, C., Gu, J., Rosenfeld, M.A., Pavan, W.J., Krizman, D.B., et al., 1997. Niemann-Pick C1 disease gene: homology to mediators of cholesterol homeostasis. Science 277 (5323), 228–231.
Casso, D., Ramirez-Weber, F.A., Kornberg, T.B., 1999. GFP-tagged balancer chromosomes for Drosophila melanogaster. Mech. Dev. 88 (2), 229–232.
Cecchini, J.P., Knibiehler, B., Mirre, C., Le Parco, Y., 1987. Evidence for a type-IV-related collagen in Drosophila melanogaster. Evolutionary constancy of the carboxyl-terminal noncollagenous domain. Eur. J. Biochem. FEBS 165 (3), 587–593.
Chen, Y., Struhl, G., 1996. Dual roles for patched in sequestering and transducing Hedgehog. Cell 87 (3), 553–563.
Cho, N.K., Keyes, L., Johnson, E., Heller, J., Ryner, L., Karim, F., Krasnow, M.A., 2002. Developmental control of blood cell migration by the Drosophila VEGF pathway. Cell 108 (6), 865–876.
Evans, I.R., Zanet, J., Wood, W., Stramer, B.M., 2010. Live imaging of Drosophila melanogaster embryonic hemocyte migrations. J. Vis. Exp. JoVE 36.
Fessler, J.H., Fessler, L.I., 1989. Drosophila extracellular matrix. Annu. Rev. Cell Biol. 5, 309–339.
Fogerty, F.J., Fessler, L.I., Bunch, T.A., Yaron, Y., Parker, C.G., Nelson, R.E., Brower, D.L., Gullberg, D., Fessler, J.H., 1994. Tiggrin, a novel Drosophila extracellular matrix protein that functions as a ligand for Drosophila alpha PS2 beta PS integrins. Development 120 (7), 1747–1758.
Franc, N.C., Dimarcq, J.L., Lagueux, M., Hoffmann, J., Ezekowitz, R.A., 1996. Croquemort, a novel Drosophila hemocyte/macrophage receptor that recognizes apoptotic cells. Immunity 4 (5), 431–443.
Franc, N.C., Heitzler, P., Ezekowitz, R.A., White, K., 1999. Requirement for croquemort in phagocytosis of apoptotic cells in Drosophila. Science 284 (5422), 1991–1994.
Ghanim, M., White, K.P., 2006. Genotyping method to screen individual Drosophila embryos prior to RNA extraction. BioTechniques 41 (4), 414, 416, 418.
Graveley, B.R., Brooks, A.N., Carlson, J.W., Duff, M.O., Landolin, J.M., Yang, L., Artieri, C.G., van Baren, M.J., Boley, N., Booth, B.W., et al., 2011. The developmental transcriptome of Drosophila melanogaster. Nature 471 (7339), 473–479.
Hampton, R.Y., 2002. Proteolysis and sterol regulation. Annu. Rev. Cell Dev. Biol. 18, 345–378.
Heino, T.I., Karpanen, T., Wahlstrom, G., Pulkkinen, M., Eriksson, U., Alitalo, K., Roos, C., 2001. The Drosophila VEGF receptor homolog is expressed in hemocytes. Mech. Dev. 109 (1), 69–77.
Hooper, J.E., Scott, M.P., 1989. The Drosophila patched gene encodes a putative membrane protein required for segmental patterning. Cell 59 (4), 751–765.
Ingham, P.W., Taylor, A.M., Nakano, Y., 1991. Role of the Drosophila patched gene in positional signalling. Nature 353 (6340), 184–187.
Kusche-Gullberg, M., Garrison, K., MacKrell, A.J., Fessler, L.I., Fessler, J.H., 1992. Laminin A chain: expression during Drosophila development and genomic sequence. EMBO J. 11 (12), 4519–4527.
Kuwabara, P.E., Labouesse, M., 2002. The sterol-sensing domain: multiple families, a unique role? Trends Genet. TIG 18 (4), 193–201.
Le Parco, Y., Knibiehler, B., Cecchini, J.P., Mirre, C., 1986. Stage and tissue-specific expression of a collagen gene during Drosophila melanogaster development. Exp. Cell Res. 163 (2), 405–412.
Manaka, J., Kuraishi, T., Shiratsuchi, A., Nakai, Y., Higashida, H., Henson, P., Nakanishi, Y., 2004. Draper-mediated and phosphatidylserine-independent phagocytosis of apoptotic cells by Drosophila hemocytes/macrophages. J. Biol. Chem. 279 (46), 48466–48476.
Mirre, C., Cecchini, J.P., Le Parco, Y., Knibiehler, B., 1988. De novo expression of a type IV collagen gene in Drosophila embryos is restricted to mesodermal derivatives and occurs at germ band shortening. Development 102 (2), 369–376.
Nybo, K., 2012. Molecular biology techniques Q&A. Western blot: protein migration. BioTechniques 53 (1), 23–24.
Olofsson, B., Page, D.T., 2005. Condensation of the central nervous system in embryonic Drosophila is inhibited by blocking hemocyte migration or neural activity. Dev. Biol. 279 (1), 233–243.
Pastenes, L., Ibanez, F., Bolatto, C., Pavez, L., Cambiazo, V., 2008. Molecular characterization of a novel patched-related protein in Apis mellifera and Drosophila melanogaster. Arch. Insect Biochem. Physiol. 68 (3), 156–170.
Rath, A., Glibowicka, M., Nadeau, V.G., Chen, G., Deber, C.M., 2009. Detergent binding explains anomalous SDS-PAGE migration of membrane proteins. Proc. Natl. Acad. Sci. U. S. A. 106 (6), 1760–1765.
Robertson, H.M., Preston, C.R., Phillis, R.W., Johnson-Schlitz, D.M., Benz, W.K., Engels, W.R., 1988. A stable genomic source of P element transposase in Drosophila melanogaster. Genetics 118 (3), 461–470.
Schmid, A., Schindelholz, B., Zinn, K., 2002. Combinatorial RNAi: a method for evaluating the functions of gene families in Drosophila. Trends Neurosci. 25 (2), 71–74.
Sears, H.C., Kennedy, C.J., Garrity, P.A., 2003. Macrophage-mediated corpse engulfment is required for normal Drosophila CNS morphogenesis. Development 130 (15), 3557–3565.
Seegmiller, A.C., Dobrosotskaya, I., Goldstein, J.L., Ho, Y.K., Brown, M.S., Rawson, R.B., 2002. The SREBP pathway in Drosophila: regulation by palmitate, not sterols. Dev. Cell 2 (2), 229–238.
Stronach, B.E., Renfranz, P.J., Lilly, B., Beckerle, M.C., 1999. Muscle LIM proteins are associated with muscle sarcomeres and require dMEF2 for their expression during Drosophila myogenesis. Mol. Biol. Cell 10 (7), 2329–2342.
Taipale, J., Cooper, M.K., Maiti, T., Beachy, P.A., 2002. Patched acts catalytically to suppress the activity of Smoothened. Nature 418 (6900), 892–897.
Taylor, A.M., Nakano, Y., Mohler, J., Ingham, P.W., 1993. Contrasting distributions of patched and hedgehog proteins in the Drosophila embryo. Mech. Dev. 42 (1–2), 89–96.
Tepass, U., Fessler, L.I., Aziz, A., Hartenstein, V., 1994. Embryonic origin of hemocytes and their relationship to cell death in Drosophila. Development 120 (7), 1829–1837.

Witsch-Baumgartner, M., Loffler, J., Utermann, G., 2001. Mutations in the human DHCR7 gene. Hum. Mutat. 17 (3), 172–182.
Wood, W., Jacinto, A., 2007. Drosophila melanogaster embryonic haemocytes: masters of multitasking. Nat. Rev. Mol. Cell Biol. 8 (7), 542–551.
Wood, W., Faria, C., Jacinto, A., 2006. Distinct mechanisms regulate hemocyte chemotaxis during development and wound healing in Drosophila melanogaster. J. Cell Biol. 173 (3), 405–416.
Wright, T.R., 1960. The phenogenetics of the embryonic mutant, lethal myospheroid, in Drosophila melanogaster. J. Exp. Zool. 143, 77–99.
Yarnitzky, T., Volk, T., 1995. Laminin is required for heart, somatic muscles, and gut development in the Drosophila embryo. Dev. Biol. 169 (2), 609–618.
Yasothornsrikul, S., Davis, W.J., Cramer, G., Kimbrell, D.A., Dearolf, C.R., 1997. viking: identification and characterization of a second type IV collagen in Drosophila. Gene 198 (1–2), 17–25.
Yoshida, H., Fuwa, T.J., Arima, M., Hamamoto, H., Sasaki, N., Ichimiya, T., Osawa, K., Ueda, R., Nishihara, S., 2008. Identification of the Drosophila core 1 beta1,3-galactosyltransferase gene that synthesizes T antigen in the embryonic central nervous system and hemocytes. Glycobiology 18 (12), 1094–1104.
Zanet, J., Stramer, B., Millard, T., Martin, P., Payre, F., Plaza, S., 2009. Fascin is required for blood cell migration during Drosophila embryogenesis. Development 136 (15), 2557–2565.
Zugasti, O., Rajan, J., Kuwabara, P.E., 2005. The function and expansion of the Patched- and Hedgehog-related homologs in C. elegans. Genome Res. 15 (10), 1402–1410.
Zuniga, A., Hodar, C., Hanna, P., Ibanez, F., Moreno, P., Pulgar, R., Pastenes, L., Gonzalez, M., Cambiazo, V., 2009. Genes encoding novel secreted and transmembrane proteins are temporally and spatially regulated during Drosophila melanogaster embryogenesis. BMC Biol. 7, 61.